Published in final edited form as:
Nat Chem. 2017 April ; 9(4): 303–309. doi:10.1038/nchem.2664.

A prebiotically plausible synthesis of pyrimidine β-ribonucleosides and their phosphate derivatives involving photoanomerization

Jianfeng Xu[1], **Maria Tsanakopoulou**[1], **Christopher J. Magnani**[1], **Rafał Szabla**[2,*], **Judit E. Šponer**[2,3], **Jiří Šponer**[2,3], **Robert W. Góra**[4], and **John D. Sutherland**[1,*]

[1]MRC Laboratory of Molecular Biology, Francis Crick Avenue, Cambridge Biomedical Campus, Cambridge CB2 0QH, UK [2]Institute of Biophysics, Academy of Sciences of the Czech Republic, Královopolská 135, 61265, Brno, Czech Republic [3]CEITEC – Central European Institute of Technology, Masaryk University, Campus Bohunice, Kamenice 5, CZ-62500 Brno, Czech Republic [4]Department of Physical and Quantum Chemistry, Faculty of Chemistry, Wrocław University of Technology, Wybrzeże Wyspiańskiego 27, 50-370 Wrocław, Poland

Abstract

Previous research into the prebiotic synthesis of the pyrimidine nucleotides has revealed a potential intermediate with remarkable properties – ribose aminooxazoline crystallises spontaneously from reaction mixtures, and with an enhanced enantiomeric excess if initially enantioenriched. This automatic chemical and chiral purification suggests that reservoirs of this compound in optically pure form might have accumulated on the early Earth. Studies have shown that ribose aminooxazoline can be efficiently converted to α-ribocytidine by way of 2,2'-anhydro-ribocytidine, though anomerization to β-ribocytidine by UV irradiation is extremely inefficient. Our previous work demonstrated the synthesis of pyrimidine β-ribonucleotides, but at the cost of ignoring ribose aminooxazoline and using arabinose aminooxazoline instead. Here, we describe a long sought route through ribose aminooxazoline to the pyrimidine β-ribonucleosides and their phosphate derivatives, that involves an extraordinarily efficient photoanomerisation of α-2-thioribocytidine. In addition to the canonical nucleosides, our synthesis accesses β-2-thioribouridine, a modified nucleoside found in tRNA and which enables both faster and more accurate nucleic acid template copying chemistry.

[*]Correspondence regarding the experimental work and requests for materials should be addressed to J.D.S., johns@mrc-lmb.cam.ac.uk; correspondence regarding the theoretical work should be addressed to R.S., rafal.szabla@gmail.com.

Author contributions

J.D.S. supervised the experimental research, and J.X., M.T. and C.J.M. performed the experiments. J.E.S, J.S. and R.W.G. oversaw the theoretical work which was carried out by R.S. All authors contributed intellectually as the project unfolded. J.D.S. wrote most of the paper and J.X., M.T., C.J.M. and R.S. further contributed and assembled the Supplementary Information.

Additional information

Reprints and permissions information is available online at www.nature.com/reprints.

Competing financial interests

The authors declare no competing financial interests.

Europe PMC Funders Author Manuscripts

Introduction

The first synthesis of pyrimidine ribonucleosides from aminooxazoline and anhydronucleoside intermediates dates back nearly fifty years, but suffers from an extremely low-yielding step and the questionable prebiotic availability of ribose.1 Orgel found that treatment of the cyanamide derivative of this sugar, ribose aminooxazoline **1** with cyanoacetylene **2** gave the anhydronucleoside **3** and thence α-ribocytidine **4** in good yield, but UV irradiation of the latter gave β-ribocytidine **5** in only 4% yield. Whilst the route had several attractive features, the inefficiency of this photoanomerization compounded concerns about the availability of ribose and made the route seem somewhat implausible from a prebiotic standpoint. (Fig. 1). Both the high crystallinity of ribose aminooxazoline **1** and its greater propensity to crystallise than its stereoisomers were noted by Orgel. In general, this behaviour is extremely attractive in prebiotic chemistry because it allows for spontaneous purification and accumulation of an intermediate such that subsequent synthetic steps in a sequence can occur without interference from the detritus of earlier steps. Accordingly, we were prompted to revisit this chemistry and, having found that nucleobase destruction giving ribose oxazolidinone **6** was the major photoreaction of α-ribocytidine **4**,2 thus concluded that this route to the β-ribonucleosides from ribose aminooxazoline **1** was irredeemable. We then moved on to explore routes involving 2'-stereoinversion and the *arabino*-configured intermediates arabinose aminooxazoline **7** and 2,2'-anhydro-arabinocytidine **8**.3 We found that phosphorylation of **8** occurred regioselectively on the 3'-OH group and was followed by intramolecular 2'-stereoinversion giving β-ribocytidine-2',3'-cyclic phosphate **9**. Finally, we discovered that UV irradiation of **9** caused partial conversion to the corresponding ribouridine-2',3'-cyclic phosphate **10**, rather than predominant nucleobase destruction, for subtle chemical reasons. However, although our synthesis provided both canonical pyrimidine ribonucleoside-2',3'-cyclic phosphates **9** and **10** in good yield, we had concerns about our reliance on arabinose aminooxazoline **7** as an intermediate.

We were further motivated to explore this area of chemistry in more detail because we had also found that pentose cyanamide derivatives can be formed in an indirect way that avoids the requirement for the free pentoses, which are unstable and difficult to access. Thus, all four pentose aminooxazolines are formed by reaction of glyceraldehyde **11** with 2 aminooxazole **12**, another compound that has desirable purification capabilities, subliming readily.4 Although ribose aminooxazoline **1** (44% yield) and arabinose aminooxazoline **7** (30% yield) greatly predominate, and are thus on the face of it equally plausible as ribonucleotide precursors, **1** selectively crystallises from the product solution. Augmenting earlier observations that this crystallisation provides a potential means whereby ribose aminooxazoline **1** might be chemically purified,1 we also found that it allows enantiomeric enrichment if the input glyceraldehyde is non-racemic. This is because **1** behaves as a true conglomerate (different enantiomers forming separate crystals or crystalline domains such that solid phase enantiomeric excesses are enhanced over those in residual material in solution).4 Although we also found that **1** can be partly epimerized to arabinose aminooxazoline **7** in phosphate buffer – presumably, on the basis of the mechanism, without loss of enantiomeric purity – the latter is the minor stereoisomer at equilibrium.5 Accordingly, we felt that enantiomerically pure ribonucleotides would most plausibly derive

from ribose aminooxazoline **1** if a route therefrom that avoided arabinose aminooxazoline **7** could be found.

Results and discussion

We recently discovered a synthetic route from hydrogen cyanide to the sugars needed for assembly of ribose aminooxazoline **1** based on reductive homologation with photochemically generated hydrated electrons.6,7 Hydrosulfide, the conjugate base of hydrogen sulfide ($pK_a = 7.2$), turned out to be the ideal source of these electrons.7 Hydrogen sulfide is a constituent of volcanic exhalations and hydrosulfide can be produced by dissolution of metal sulfides in cyanide solution.7 Given their availability and their involvement in the photochemical synthesis of the constituents of ribose aminooxazoline **1**, we wondered if these sulfur species and irradiation might also play a role in the further conversion of **1** to ribonucleotides. For the sake of clarity, we present our findings before we discuss the mechanisms and implication of the reactions we uncovered.

Formation, photoanomerization and hydrolysis of thionucleosides

We first sought an inherently favoured reaction of ribose aminooxazoline **1**, or one of its derivatives, with hydrosulfide and, in this way, discovered that the anhydronucleoside **3** undergoes smooth thiolysis8 in aqueous formamide giving α-2-thioribocytidine **13** in 84% yield along with the hydrolysis product α-ribocytidine **4** in 16% yield (Figs. 2 & 3a–c, Supplementary Figs. 30 & 31). We then investigated the UV photoanomerization of α-2-thioribocytidine **13** and found that it took place extremely efficiently to give β-2-thioribocytidine **14** in 76% yield (Figs. 2 & 3c–e, Supplementary Figs. 32–34). Small amounts of starting material (11%) remained after irradiation at 254nm for 2.5 days (in aqueous solution containing hydrogen sulfide to minimize photooxidation by adventitious oxygen) and there was also low level nucleobase loss (thiocytosine **15** detected in 4% yield) and hydrolysis to α-ribocytidine **4** (9%).

We then investigated hydrolysis of the 2-thioribocytidine nucleosides **13** and **14** and further chemistry of the hydrolysis products. Mild acid hydrolysis of α-2-thioribocytidine **13** in dilute formic acid (40 mM, pH = 3, 60°C) gave α-2-thioribouridine **16** in 93% yield after 14 days (Supplementary Figs. 36 & 37), whereas the hydrolysis of β-2-thioribocytidine **14** under the same conditions was slower and less selective giving β-2-thioribouridine **17** in 38% yield after 54 days along with products of nucleobase loss (2-thiocytosine **15**, 34%; 2-thiouracil **18**, 18% and ribose) (Supplementary Figs. 39 & 40). In contrast to what we found in the 2-thiocytidine series, photoanomerization of α-2-thioribouridine **16** to β-2-thioribouridine **17** was not observed, rather there was extensive nucleobase destruction resulting in the liberation of ribose (Supplementary Fig. 35). Hydrolysis of β-2-thioribocytidine **14** at pH = 7 in the presence of phosphate buffer (100 mM, 60°C) was slow, but after 84 days, cleanly furnished the canonical nucleoside β-ribocytidine **5** (41%, Figs. 2 & 3e–g, Supplementary Figs. 41 & 42) along with small amounts of β-2-thioribouridine **17** (2%) and β-ribouridine **19** (3%) produced by the very slow hydrolysis of **5** itself.9 Hydrolysis at pH = 5 in the presence of phosphate buffer (100 mM, 60°C) for a similar length of time gave more β-2-thioribouridine **17** (8%) and less β-ribocytidine **5** (33%).

Although we only monitored the hydrolysis of β-2-thioribocytidine **14** for about one half-life at pH = 7 and pH = 5, more β-ribocytidine **5**, β-ribouridine **19** and β-2-thioribouridine **17** would be produced after longer periods.

Phosphorylation

Prebiotically plausible phosphorylation of nucleosides has been demonstrated in hot formamide solution and in urea melts.10,11 Although the 5'-monophosphates or the 2',3'-cyclic phosphates of the β-ribopyrimidine nucleosides **5** and **19** can be formed this way depending on the conditions,11 we also investigated the direct phosphorylation of β-2-thioribocytidine **14**. Somewhat surprisingly, the 2',3'-cyclic phosphate of the 2-thiocytidine nucleoside was not detected when **14** was allowed to react with inorganic phosphate in hot formamide. Instead, β-ribocytidine **5** (48%) and its 2',3'-cyclic-phosphate derivative **9** (24%) were detected along with 2,4-diaminopyrimidine **20** (21%) (Supplementary Figs. 43–46). Since it has previously been shown that UV irradiation partly converts **9** to its uridine analogue **10**,3 the direct phosphorylation of β-2-thioribocytidine **14** can therefore lead to both canonical β-ribopyrimidine nucleoside 2',3'-cyclic phosphates **9** and **10**.

Thiolysis mechanism

Mechanistically, thiolysis of the anhydronucleoside **3** presumably involves repeated reversible nucleophilic attack at C-2 by hydrosulfide followed by occasional extrusion of O-2' from the tetrahedral intermediate thus formed giving α-2-thioribocytidine **13**. Although water or hydroxide are less nucleophilic than hydrosulfide, extrusion of O-2' from the tetrahedral intermediate formed by addition of these oxygenous nucleophiles to the anhydronucleoside **3** must be a common event and this is probably one of the reasons why thiolysis of **3** is accompanied by hydrolysis to α-ribocytidine **4**. The hydrolysis might also be subject to general base catalysis by hydrosulfide. As solvent for subsequent phosphorylation chemistry, we envisioned using formamide – the hydration product of hydrogen cyanide. We therefore also evaluated aqueous formamide for the thiolysis step and found it to allow smooth conversion of the anhydronucleoside **3** to α-2-thioribocytidine **13** with minimal competing hydrolysis. In the phosphorylation step, the formamide solvent has to be essentially anhydrous and this can easily be plausibly achieved simply by heating.

The pH dependence of the hydrolysis of β-2-thioribocytidine **14** is presumably due to the relative electrophilicities of C-2 and C-4 depending on the protonation state of **14**, and relative leaving group abilities. At low pH, ammonia can be lost from a tetrahedral intermediate formed by nitrogen protonation and attack of water at C-4 of **14** (or the reversibly formed 5,6-double bond hydration adduct thereof), whereas at neutral pH, hydrosulfide can be lost from a more rarely accessed tetrahedral intermediate formed by attack of water or hydroxide at C-2. The more rapid dilute acid hydrolysis of α-2-thioribocytidine **13** is due to neighbouring group participation by the 2'-OH and a tricyclic intermediate could be detected by ^{1}H-NMR spectroscopy during the hydrolysis (Supplementary Figs. 37 & 38).

Phosphorylation mechanism

A mechanism for the photochemical conversion of α-2-thioribocytidine **13** to the β-anomer **14** was not immediately apparent, and further experimental and computational investigations of this key reaction were carried out as described below. However, conventional organic reasoning did explain the behaviour of **14** under phosphorylation conditions (Fig. 4a). Reversible phosphorylation in hot formamide is thought to involve formidoylphosphate **21** formed by dissociative nucleophilic displacement of water from a rare tautomer of the phosphate monoanion (Fig. 4a, inset box). The ability of formamide to displace an oxygenous leaving group from a phosphorus atom in such a molecular context means that if phosphate adds to an electrophilic carbon and then undergoes attack by formamide, an oxygen atom is delivered to the electrophilic carbon. Thus, on heating with inorganic phosphate in formamide, β-2-thioribocytidine **14** can either undergo phosphorolytic loss of hydrogen sulfide to give β-ribocytidine **5 –** which can then undergo reversible phosphorylation to give β-ribocytidine-2',3'-cyclic phosphate **9** – or be directly phosphorylated to the thermodynamically favoured β-2-thioribocytidine-2',3'-cyclic phosphate **22**. Intermolecular phosphorolytic loss of hydrogen sulfide from **22** giving β-ribocytidine-2',3'-cyclic phosphate **9** is then possible. However, the 2',3'-cyclic phosphate ring of **22** constrains the sugar's conformational preferences12 such that intramolecular addition of the 5'-OH group to C-2 of the nucleobase with loss of hydrogen sulfide additionally becomes possible. The 2,5'-anhydronucleotide **23** that results is susceptible to phosphorolytic cleavage to give β-ribocytidine-2',3'-cyclic phosphate **9,** and to aminolysis – by ammonia produced by α-elimination from formamide – giving the 2,4-diaminopyrimidine cyclic nucleotide **24**. Glycosidic bond cleavage of **24** is then presumed to be facile because of the basicity of the nucleobase,13 and the enhanced leaving group ability of the protonated nucleobase. This cleavage would generate the free 2,4-diaminopyrimidine **20** that we observed, and an unstable sugar moiety prone to decompose to a slew of products that we did not observe – presumably because of the low yield of each individual product.

Photoanomerization mechanism

We then turned our attention to the mechanism of photoanomerization of α-2-thioribocytidine **13**, and further sought an explanation as to why α-2-thioribouridine **16** did not undergo similar epimerization upon irradiation. Suspecting an interrupted Norrish type II reaction similar to that we observed for the photoanomerization of 2'-deoxycytidine,14 we irradiated α-2-thioribocytidine **13** in D_2O since anomerization by this mechanism would (presumably) be associated with deuterium incorporation at C-1'. Gratifyingly, after 12 hours irradiation we observed complete deuterium incorporation at C-1' of the product, β-2-thioribocytidine **14** and of the residual starting material **13** demonstrating that exchange is faster than anomerization (Fig. 4b,c). Furthermore, by 36 hours the reaction appeared to reach equilibrium with the β-and α-isomers in a ratio of 85:15 – as calculated using relative integrations of signals due to H-6 of both anomers in the ^{1}H-NMR spectrum of the crude reaction products (Supplementary Fig. 47). To confirm the equilibrium, the β-isomer was irradiated in D_2O whereupon conversion to the α-isomer and C-1' deuteration were observed and, after 36 hours equilibrium had again been reached ((Fig. 4d,e, Supplementary Fig. 48) β-and α-isomers in a ratio of 88:12). In further support of the proposed mechanism, the

deuterated anomers were purified from a preparative scale UV reaction and characterised by NMR and LCMS (See Supplementary Information).

Photoanomerization theory

Deuterium incorporation at the C-1' carbon atom is consistent with 2-thioribocytidine **13/14** undergoing photoanomerization via excited state C1'–H atom abstraction by the C=S group (Fig. 5a,b). The intermediate α-/β-**25** formed after the hydrogen abstraction possesses an SH group which can readily exchange the proton with a deuteron from surrounding D_2O molecules. The SD group thus formed can subsequently deliver this deuteron to the C-1' position before or after anomerization through C1' radical inversion. In the case of 2'-deoxycytidine, the excited-state H-atom abstraction reaction occurs on the hypersurface of the lowest-lying nπ* singlet state (S_1). The minima of the S_1 states of both 2-thioribocytidine **13/14** and 2-thioribouridine **16/17** are of nπ* character and according to our calculations the S_1/S_0 state crossing related to this process is energetically accessible in both molecules. However, it is worth noting that the presence of sulfur significantly enhances spin-orbit couplings (SOCs) in organic molecules, and in consequence may enable very efficient non-radiative transitions to the triplet manifold. 15–17 In particular, it was shown that thiothymidines, 6-thioguanine and 2-thiouracil undergo ultrafast intersystem crossing (ISC) resulting in near unity triplet yields.17,18 Our estimates of intersystem crossing (ISC) rates suggest that the photoanomerization of 2-thioribocytidine **13/14** may occur predominantly on the triplet hypersurface.

The initially populated excited state of 2-thioribocytidine **13/14** may undergo barrierless vibrational relaxation towards the minimum on the corresponding S_1 potential energy surface (Fig. 5b). Since the minimum-energy structure of the T_1 state of 2-thioribocytidine is also of nπ* character, the corresponding $^1n\pi^*(S_1)\rightarrow{}^3n\pi^*(T_1)$ intersystem crossing (ISC) operates without molecular orbital change and should be rather slow according to the El-Sayed rules and the results of our calculations. Therefore we suggest (based on reasoning given in the Supplementary Information) that the primary ISC channel is most likely related to the $^1n\pi^*(S_1)\rightarrow{}^3\pi\pi^*(T_2)$ transition. The T_1 state can then be accessed almost immediately after the $S_1\rightarrow T_2$ ISC since at the S_1/T_2 minimum energy crossing point the T_2 and T_1 states are almost degenerate (yielding a $S_1/T_2/T_1$ three-state crossing). The H-atom abstraction can then take place in the T_1 state and when the S–H distance approaches 1.55 Å, the T_1 and S_0 (ground) electronic states cross.

Similarly, as found for 2-thiouracil,17,19,20 the T_1 state of 2-thioribouridine **16/17** has a ππ* character and it can be more efficiently accessed from the S_1 state due to large SOCs between these two states. However, H-abstraction is not possible on the surface of the $^3\pi\pi^*$ state and consequently, the S_0 and T_1 surfaces correlate adiabatically and do not cross (Fig. 3g, inset box). The T_1/S_0 state crossing can be accessed along the H-abstraction coordinate only after the change of the T_1 character from $^3\pi\pi^*$ to $^3n\pi^*$, which is related to an energy barrier of 0.84 eV in the gas phase. This energy barrier is presumably even higher in bulk water due to destabilization of nπ* states in aqueous environment (see the Supplementary Information).21 Furthermore, the C=S....H–C1' distance is significantly larger in the T_1 minimum of 2-thioribouridine **16/17** (2.65 Å) than in the respective minimum of 2-

thioribocytidine **13/14** (2.43 Å), which should significantly affect the accessibility of this reaction pathway. Therefore, we conclude that photoanomerization via an interrupted Norrish type II reaction in the triplet manifold is clearly hindered in the case of 2-thiouridine. Unable to lose energy by T_1/S_0 state crossing along the H-abstraction coordinate and subsequent vibrational relaxation, the $^3\pi\pi^*$ state undergoes other, as yet undefined, photochemistry that results in nucleobase destruction and liberation of ribose.

Conclusions

The route to the canonical pyrimidine β-ribonucleosides **5** and **19** that we have uncovered in this work is short and high-yielding. The 5'-phosphates of **5** and **19** can be produced easily under plausible conditions, as can their 2',3'-cyclic phosphates **9** and **10**.11 The latter can alternatively be produced by irradiation of the phosphorylation products of β-2-thioribocytidine **14**. The β-ribonucleosides and nucleotides all derive from ribose aminooxazoline **1**, crystallization of which provides an opportunity for enantioenrichment because of its conglomerate behaviour. Enantiomerically pure pyrimidine β-ribonucleotides can thus be considered prebiotically plausible if a means of producing glyceraldehyde **11** with sufficient enantiomeric excess for the subsequent crystallization of **1** to give a single enantiomer is demonstrated. Having enantiomerically pure β-ribonucleotides is crucial to producing RNA by oligomerization since racemic (or even scalemic) mixtures can either be expected to produce vast numbers of diastereoisomerically isomeric oligonucleotides, or result in inhibition of oligomerization through enantiomeric cross-inhibition.22 Because different phosphorylated β-ribonucleosides can be produced, oligomerisation could result in 5'- or 2',(/)3'-phosphorylated RNA.

Finally, we note that a side product of the chemistry documented in this paper, β-2-thioribouridine **17**, and its derivatives are found in the anticodon stem loop of certain tRNAs where they are involved in split-box decoding.23 Furthermore, replacing β-ribouridine **19** with β-2-thioribouridine **17** leads to both faster and more accurate nonenzymatic template copying chemistry suggesting that **17** might have played a role in chemical RNA replication at an early stage in the origin of life.24 Taken with the foregoing, the formation of β-2-thioribocytidine **14** reported herein suggests that its role in RNA replication chemistry should also be investigated.

Supplementary Material

Refer to Web version on PubMed Central for supplementary material.

Acknowledgements

This work was supported by the Medical Research Council (No. MC_UP_A024_1009), a grant from the Simons Foundation (No. 290362 to J.D.S.), grant 14-12010S from the Grant Agency of the Czech Republic and by the project CEITEC 2020 (LQ1601) with financial support from the Ministry of Education, Youth and Sports of the Czech Republic under the National Sustainability Programme II. Support from a statutory activity subsidy from the Polish Ministry of Science and Higher Education for the Faculty of Chemistry of Wrocław University of Technology is gratefully acknowledged. Theoretical calculations were partly performed at the Wrocław Center for Networking and Supercomputing (WCSS) and Interdisciplinary Centre for Mathematical and Computational Modelling in Warsaw (ICM).

Europe PMC Funders Author Manuscripts

References

1. Sanchez RA, Orgel LE. Studies in prebiotic synthesis. Synthesis and photoanomerization of pyrimidine nucleosides. J Mol Biol. 1970; 47:531–543. [PubMed: 5418170]
2. Powner MW, et al. On the prebiotic synthesis of ribonucleotides: photoanomerisation of cytosine nucleosides and nucleotides revisited. ChemBioChem. 2007; 8:1170–1179. [PubMed: 17549787]
3. Powner MW, Gerland B, Sutherland JD. Synthesis of activated pyrimidine ribonucleotides in prebiotically plausible conditions. Nature. 2009; 459:239–242. [PubMed: 19444213]
4. Anastasi C, Crowe MA, Powner MW, Sutherland JD. Direct assembly of nucleoside precursors from two- and three-carbon units. Angew Chem Int Ed. 2006; 45:6176–6179.
5. Powner MW, Sutherland JD. Phosphate-mediated interconversion of ribo- and arabino-configured prebiotic nucleotide intermediates. Angew Chem Int Ed. 2010; 49:4641–4643.
6. Ritson D, Sutherland JD. Prebiotic synthesis of simple sugars by photoredox systems chemistry. Nature Chem. 2012; 4:895–899. [PubMed: 23089863]
7. Ritson DJ, Sutherland JD. Synthesis of aldehydic ribonucleotide and amino acid precursors by photoredox chemistry. Angew Chem Int Ed. 2013; 52:5845–5847.
8. Kawaguchi T, et al. Enzymatic reactivity and anti-tumor activity of 1-(β-D-arabinofuranosyl)-2-thiocytosine derivatives. Chem Pharm Bull. 2000; 48:454–457. [PubMed: 10783060]
9. Frick L, Mac Neela JP, Wolfenden R. Transition state stabilization by deaminases: rates of nonenzymatic hydrolysis of adenosine and cytidine. Bioorg Chem. 1987; 15:100–108.
10. Schoffstall AM. Prebiotic phosphorylation of nucleosides in formamide. Orig Life. 1976; 7:399–412. [PubMed: 1023139]
11. Lohrmann R, Orgel LE. Urea-inorganic phosphate mixtures as prebiotic phosphorylating agents. Science. 1971; 171:490–494. [PubMed: 5099649]
12. Saenger, W. Principles of Nucleic Acid Structure. Springer-Verlag; New York: 1984.
13. Brown DJ, Jacobsen NW. 612. Pyrimidine reactions. Part IV. The methylation of 2,4- and 4,5-diaminopyrimidine and related compounds. J Chem Soc (Resumed). 1962:3172–3179.
14. Szabla R, et al. Excited-state hydrogen atom abstraction initiates the photochemistry of β-2′-deoxycytidine. Chem Sci. 2015; 6:2035–2043. [PubMed: 27182431]
15. Mai S, Marquetand P, González L. Intersystem crossing pathways in the noncanonical nucleobase 2-thiouracil: A time-dependent picture. J Phys Chem Lett. 2016; 7:1978–1983. [PubMed: 27167106]
16. Martínez-Fernández L, Corral I, Granucci G, Persico M. Competing ultrafast intersystem crossing and internal conversion: a time resolved picture for the deactivation of 6-thioguanine. Chem Sci. 2014; 5:1336–1347.
17. Pollum M, Crespo-Hernández CE. The dark singlet state as a doorway state in the ultrafast and efficient intersystem crossing dynamics in 2-thiothymine and 2 thiouracil. J Chem Phys. 2014; 140:071101. [PubMed: 24559331]
18. Taras-Goślińska K, Burdziński G, Wenska G. Relaxation of the T_1 excited state of 2-thiothymine, its riboside and deoxyriboside-enhanced nonradiative decay rate induced by sugar substituent. J Photochem Photobiol Chem. 2014; 275:89–95.
19. Gobbo JP, Borin AC. 2-Thiouracil deactivation pathways and triplet states population. Comput Theor Chem. 2014; 1040:195–201.
20. Mai S, Marquetand P, González L. A static picture of the relaxation and intersystem crossing mechanisms of photoexcited 2-thiouracil. J Phys Chem A. 2015; 119:9524–9533. [PubMed: 26284285]
21. Besley NA, Hirst JD. Ab initio study of the electronic spectrum of formamide with explicit solvent. J Am Chem Soc. 1999; 121:8559–8566.
22. Joyce GF, Schwartz AW, Miller SL, Orgel LE. The case for an ancestral genetic system involving simple analogues of the nucleotides. Proc Natl Acad Sci USA. 1987; 84:4398–4402. [PubMed: 2440020]

23. Grosjean H, de Crécy-Lagard V, Marck C. Deciphering synonymous codons in the three domains of life: co-evolution with specific tRNA modification enzymes. FEBS Lett. 2010; 584:252–264. [PubMed: 19931533]

24. Heuberger BD, Pal A, Del Frate F, Topkar VV, Szostak JW. Replacing uridine with 2-thiouridine enhances the rate and fidelity of nonenzymatic RNA primer extension. J Am Chem Soc. 2015; 137:2769–2775. [PubMed: 25654265]

Europe PMC Funders Author Manuscripts

Europe PMC Funders Author Manuscripts

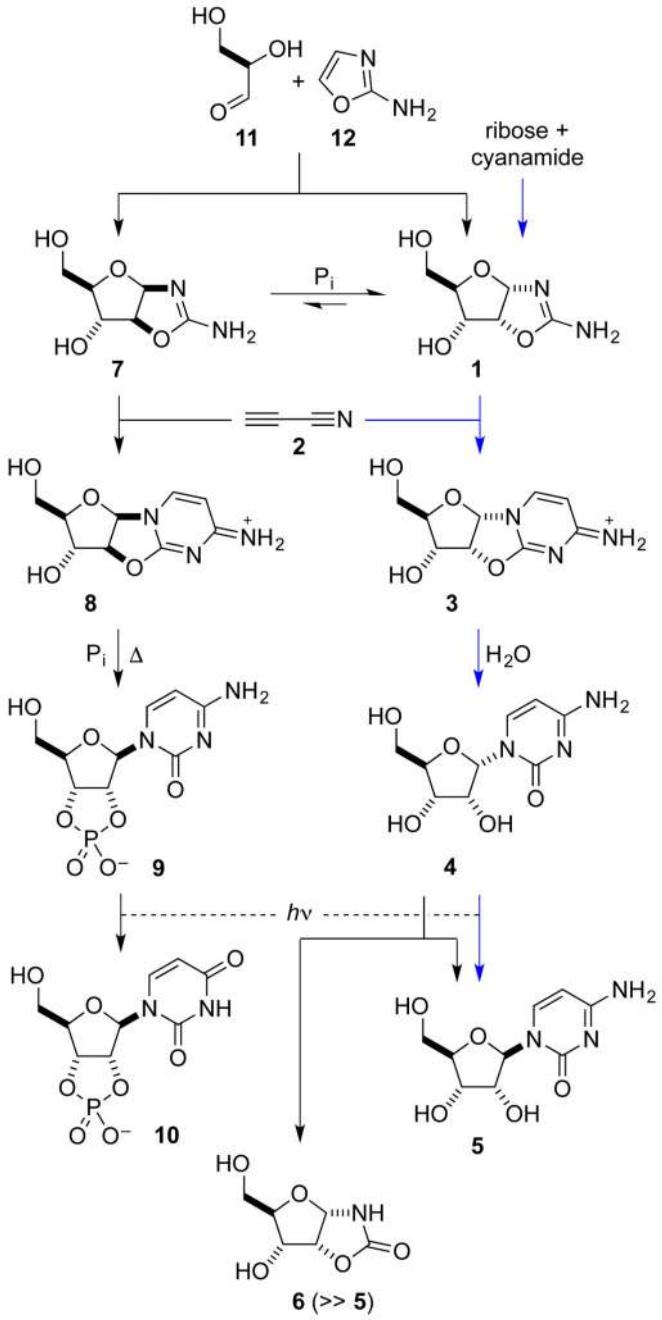

Figure 1. Previous prebiotic syntheses of pyrimidine β-ribonucleotides *via* 2,2'-anhydronucleoside intermediates.

The route initially described by Orgel is indicated by the blue arrows.1 Thus treatment of ribose with cyanamide gave a beautifully crystalline aminooxazoline **1** which underwent reaction with cyanoacetylene **2** to give the anhydronucleoside **3** and thence, by hydrolysis, α-ribocytidine **4**. However, anomerization to β-ribocytidine **5** by irradiation of **4** with UV light was very inefficient and this, along with doubts about the prebiotic provenance of ribose, lessened the attractiveness of the route. We determined that one of the reasons for the

low photoanomerization yield was competing formation of the oxazolidinone **6** and then found an alternate route to the pyrimidine ribonucleotides via the arabinose aminooxazoline **7** and anhydronucleoside **8**. The key steps were a regioselective phosphorylation and 2'-inversion reaction of **8** giving β-ribocytidine-2',3'-cyclic phosphate **9** and the partial photochemical conversion of **9** to the corrsponding uridine analogue **10**. We also found that pentose aminooxazolines, predominantly **1** and **7**, can be produced in an indirect way from glyceraldehyde **11** and 2-aminooxazole **12**. Although our route marked the first high-yielding synthesis of the pyrimidine ribonucleotides under prebiotically plausible conditions, it did not exploit the crystallinity of **1**.

Europe PMC Funders Author Manuscripts

Europe PMC Funders Author Manuscripts

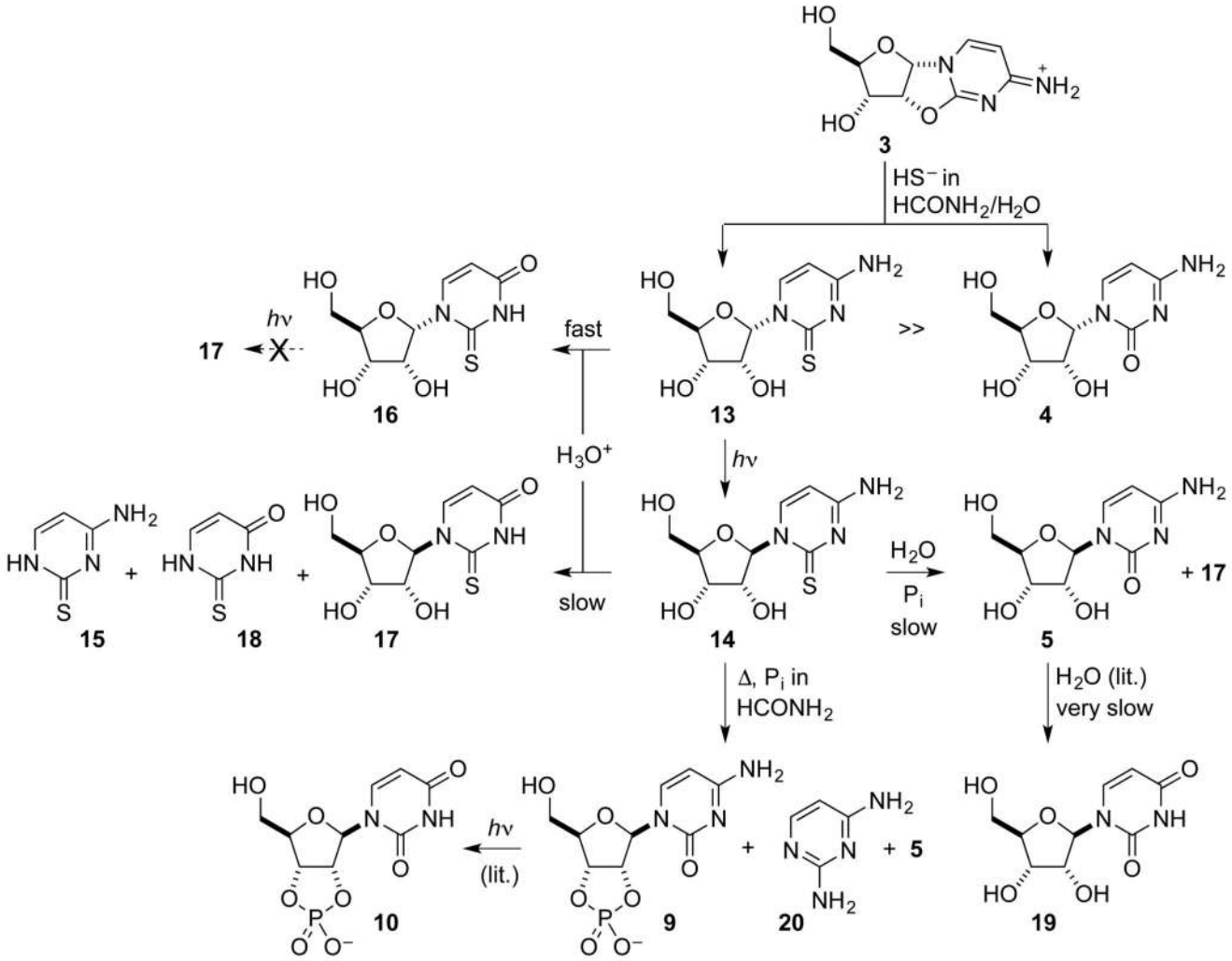

Figure 2. Synthesis of pyrimidine β-ribonucleosides and β-ribonucleotides involving photoanomerization of α-2-thioribocytidine 13.

The reaction scheme incorporates the new synthesis and the known hydrolysis of β-ribocytidine **5** to β-ribouridine **19**.9 Thiolysis of the ribose anhydronucleoside **3** gives α-2-thioribocytidine **13** in high yield along with a small amount of α-ribocytidine **4**. In marked contrast to **4**, **13** undergoes remarkably efficient photoanomerization, giving β-2-thioribocytidine **14** in excellent yield. The canonical pyrimidine ribonucleosides **5** and **19** can be produced from **14** by hydrolysis. Phosphorylation of **14** is accompanied by conversion of the 2-thiocytosine nucleobase to cytosine providing a direct route to the canonical pyrimidine ribonucleoside-2',3'-cyclic phosphates **9** and thence **10** and an alternative route to the ribonucleoside **5**. 2-Thioribouridines **16** and **17** can also be produced by hydrolysis of **13** and **14** respectively under acidic conditions.

Europe PMC Funders Author Manuscripts

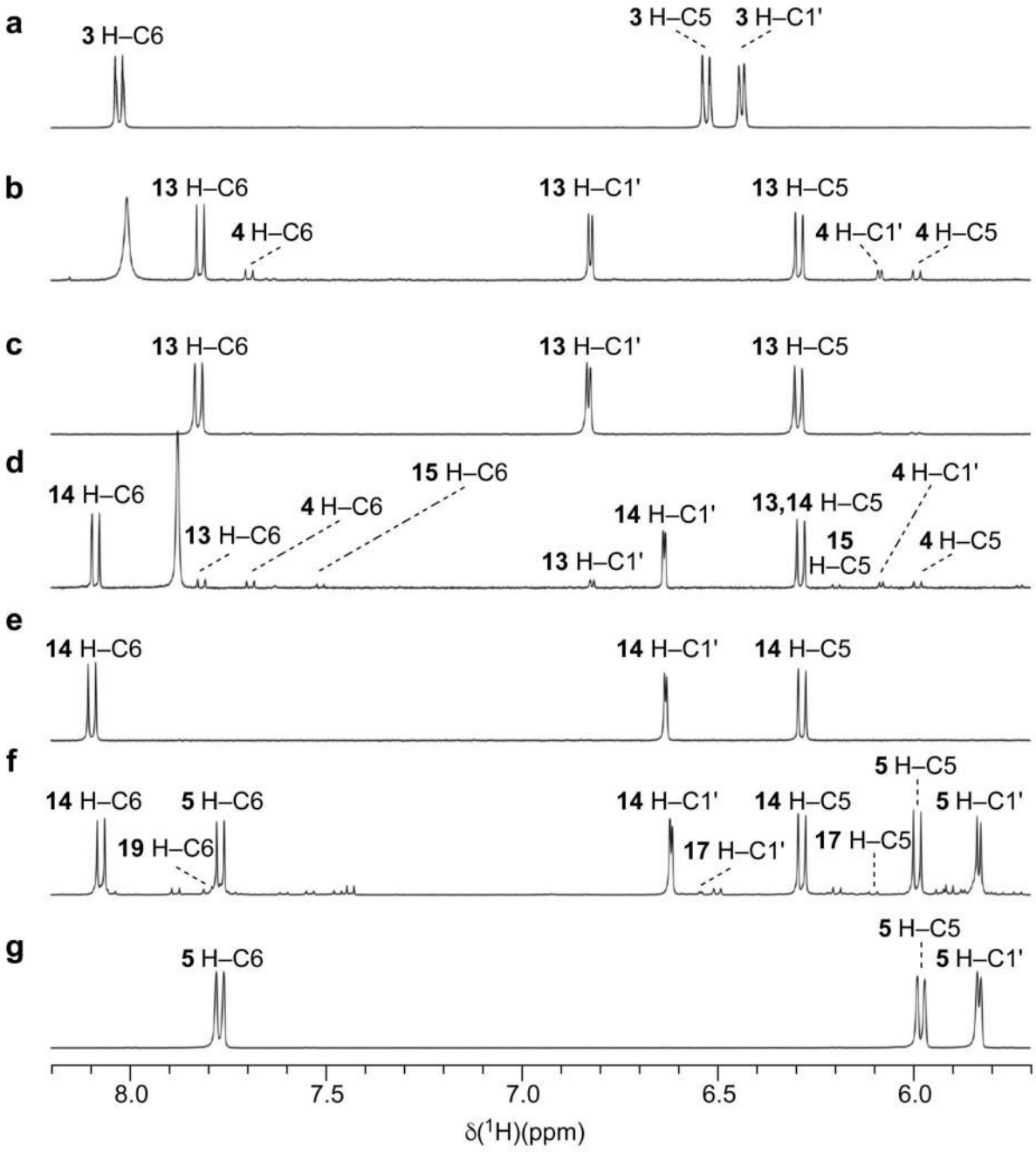

Figure 3. ^{1}H NMR spectra demonstrating the inherently favoured nature of the individual reactions of the newly discovered synthetic sequence.

^{1}H NMR spectra were recorded at 400 MHz with samples of reaction products (after removal of solvents) and synthetic standard dissolved in H_2O-D_2O **a**, Spectrum of the starting material, 2,2'-anhydro-ribocytidine **3**. **b**, Spectrum of the products of thiolysis of **3** by HS^- in wet formamide (singlet at δ ~ 8.0 ppm is due to residual formamide). Note the quantitative transformation of **3** and the predominance of α-2-thioribocytidine **13** over α-ribocytidine **4** in the products. **c**, Spectrum of an authentic sample of α-2-thioribocytidine

13. **d**, Spectrum of the products of irradiation of **13** in aqueous solution (singlet at δ ~ 7.9 ppm is due to residual dimethylformamide from the conventional synthesis of **13**). Note the remarkably clean conversion of **13** to the anomer β-2-thioribocytidine **14**. **e**, Spectrum of an authentic sample of β-2-thioribocytidine **14**. **f**, Spectrum of the products of hydrolysis of **14** in pH = 7 phosphate buffer after ~ one half life. Despite the conversion of **14** being only partial, note the clean production of β-ribocytidine **5** and the appearance of its hydrolysis product, β-ribouridine **19** as well as β-2-thioribouridine **17**, the product of alternate hydrolysis of **14**. **g**, Spectrum of an authentic sample of β-ribocytidine **5**.

Europe PMC Funders Author Manuscripts

Europe PMC Funders Author Manuscripts

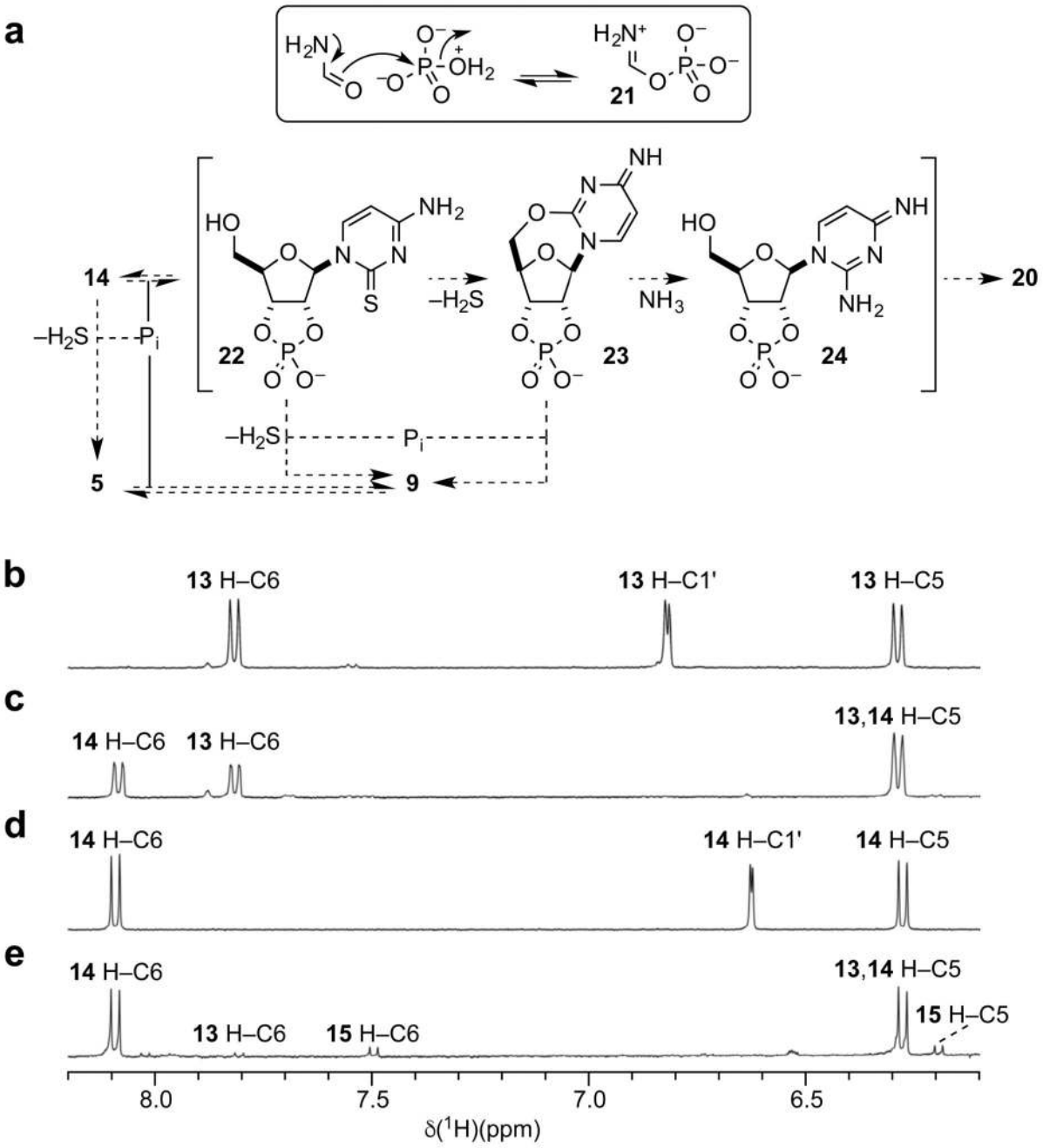

Figure 4. Reaction mechanisms.

a, Mechanisms of phosphorylation and the degradation of β-2-thioribocytidine-2',3'-cyclic phosphate **22**. The generation of the active phosphorylating agent, formidoyl phosphate **21**, in the phosphorylation of β-2-thioribocytidine **14** is shown in the box – the phosphorylation of **14** itself involves a hydroxyl group thereof attacking the imidoyl phosphate in a manner analogous to the reverse of the electron movements indicated by the arrows. Outside of the box, the mechanisms of the reactions taking place during the phosphorylation of β-2-thioribocytidine **14** are shown. **b–e**, ^{1}H NMR spectra (400 MHz, H_2O-D_2O) demonstrating

incorporation of deuterium at at C-1' of α/β-2-thioribocytidine **13/14** during photoanomerization. **b**, Expansion of the spectrum of α-2-thioribocytidine **13** showing signals for H-6, H-1' and H-5. **c**, Spectrum of the products of irradiation of α-2-thioribocytidine **13** in D_2O for 12 hours showing signals for H-6 and H-5 of both **13** and β-2-thioribocytidine **14** but lacking signals for H-1' of either anomer. **d**, Spectrum of **14** prior to irradiation. **e**, Spectrum of the products of irradiation of **14** in D_2O for 36 hours. The deuteration data shown indicate a mechanism of photoanomerization involving exchange of H-1' with solvent.

Europe PMC Funders Author Manuscripts

Europe PMC Funders Author Manuscripts

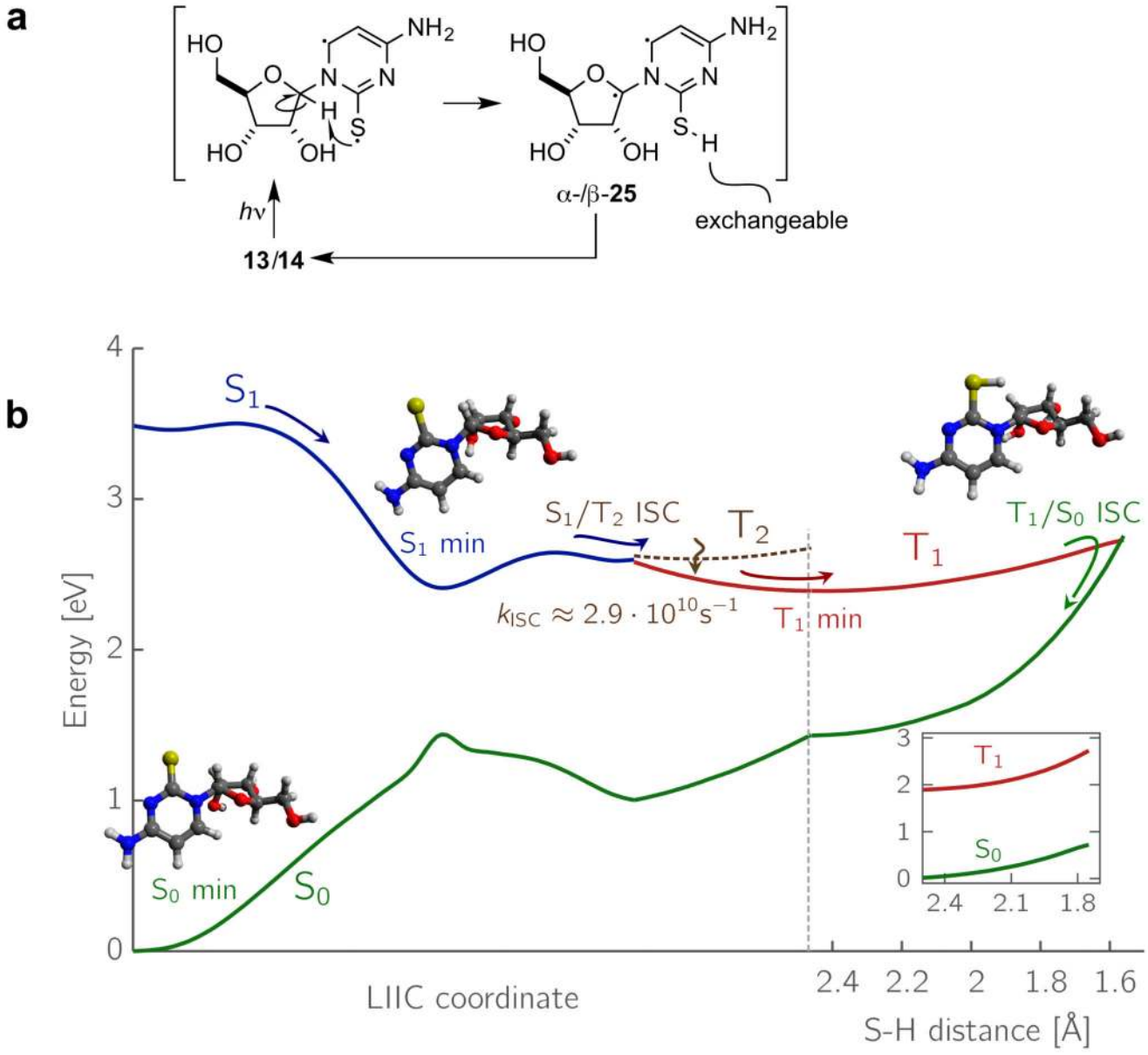

Figure 5. Mechanism of the key photoanomerization reaction.

a, Conventional organic chemical depiction of the mechanism of the photoanomerization of α/β-2-thioribocytidine **13/14** via the diradical **25**. **b**, The same mechanism but analysed at a deeper level to explain the niceties of the reaction. Potential energy (PE) profiles presenting the photoanomerization reaction of α-2-thioribocytidine. The PE cuts on the left-hand side were obtained by interpolations between the Franck-Condon region, S_1 minimum, S_1/T_2 minimum energy crossing point and the T_1 minimum. The PE profile on the right was obtained from a relaxed scan along the S–H distance. The inset box on the right corresponds to the relaxed scan along the S–H distance of α-2-thioribouridine, for which the $T_1(\pi\pi^*)$ and S_0 states do not cross. The energies were calculated using the ADC(2)/cc-pVTZ method and the computations of the SOC matrix elements were performed at the CASPT2/CASSCF

level (employing cc-pVTZ-DK basis set). Details of the S_1/T_2 intersystem crossing rate constant computations can be found in the Supplementary Information.

Europe PMC Funders Author Manuscripts